Med Biol Eng Comput (2013) 51:799–809
DOI 10.1007/s11517-013-1050-9

ORIGINAL ARTICLE

Non-linear adaptive controllers for an over-actuated pneumatic MR-compatible stepper

Christoph Hollnagel · Heike Vallery · Rainer Schädler · Isaac Gómez-Lor López · Lukas Jaeger · Peter Wolf · Robert Riener · Laura Marchal-Crespo

Received: 6 November 2012 / Accepted: 8 February 2013 / Published online: 22 February 2013

Abstract Pneumatics is one of the few actuation principles that can be used in an MR environment, since it can produce high forces without affecting imaging quality. However, pneumatic control is challenging, due to the air high compliance and cylinders non-linearities. Furthermore, the system's properties may change for each subject. Here, we present novel control strategies that adapt to the subject's individual anatomy and needs while performing accurate periodic gait-like movements with an MRI compatible pneumatically driven robot. In subject-passive mode, an iterative learning controller (ILC) was implemented to reduce the system's periodic disturbances. To allow the subjects to intend the task by themselves, a zero-force controller minimized the interaction forces between subject and robot. To assist patients who may be too weak, an assist-as-needed controller that adapts the assistance based on online measurement of the subject's performance was designed. The controllers were experimentally tested. The ILC successfully learned to reduce the variability and tracking errors. The zero-force controller allowed subjects to step in a transparent environment. The assist-as-needed controller adapted the assistance based on individual needs, while still challenged the subjects to perform the task. The presented controllers can provide accurate pneumatic control in MR environments to allow assessments of brain activation.

Keywords Pneumatic actuation · Iterative learning control · Assist-as-needed · MR compatible robots

C. Hollnagel · H. Vallery · R. Schädler · I. G.-L. López · L. Jaeger · P. Wolf · R. Riener · L. Marchal-Crespo (✉)
Sensory-Motor Systems (SMS) Lab, Institute of Robotics and Intelligent Systems (IRIS), ETH Zurich, Zurich, Switzerland
e-mail: laura.marchal@hest.ethz.ch

C. Hollnagel
e-mail: christoph.hollnagel@gmx.de

H. Vallery
Biomedical Engineering, Khalifa University of Science, Technology and Research, Abu Dhabi, UAE

R. Riener · L. Marchal-Crespo
Medical Faculty, Balgrist University Hospital, University of Zurich, Zurich, Switzerland

1 Introduction

There is increasing interest in using robotic devices to provide rehabilitation therapy following neurologic injuries [23]. The most largely administered robotic therapy comprises assistive exercises that use physical assistance to help patients to perform the rehabilitation movements. Patient's effort during physical training is thought to be an important factor in order to provoke motor plasticity [22, 25], hence robotic devices could potentially decrease recovery if they encourage a decrease in effort, energy consumption, or attention during training [19]. Previous research indicates that robotic therapy devices should be designed to assist as needed: provide just enough assistance to allow patients to practice the task, while decreasing their assistance, encouraging individuals to execute the movement on their own [10, 24, 27].

The effect of rehabilitation training on neuronal circuits in the brain is not fully understood. Further, it is still unclear how different rehabilitation strategies contribute to restorative processes of the central nervous system [29]. Knowledge about the effects of rehabilitation on neuroplasticity could help to improve the efficiency of

rehabilitation. Such knowledge can be gained by monitoring brain activation during well controlled and repeated movements. The method of choice to monitor brain activation is functional magnetic resonance imaging (fMRI), as it is non-invasive, harmless, and provides a high spatial resolution [1]. In the scanner, the desired movement should be guided by a closed-loop controlled robotic device to both guarantee repeatability of movements in subject-passive mode, and to enable measurements of movements and forces performed by the subject in a subject-active mode. Furthermore, the robot should be able to assist-as-needed, i.e., the device should be able to adapt the controller parameters based on online measurements of the participant's performance.

Several technical components are available to actuate devices in the MR environment or to transmit forces into it: pneumatic cylinders and stepper motors have been employed [5, 13, 33] as well as hydraulic cylinders with long tubes, in standard [34, 35] or in master–slave configurations [15, 16]. In addition, forces and movements have been transmitted via cables [3] or produced by ultrasonic motors [4, 14], electro-rheological fluids [20, 21], and special electromagnetic principles [28]. These technical approaches have been applied mostly in the field of surgery [4, 12, 26], placement of biopsy needles in the scanner [9, 17], and mapping brain activity during functional movements and rehabilitation [21, 30, 32].

Generation of gait-like movements is particularly challenging due to the subject's supine position and the limited space in the scanner. Therefore, the gait movement needs to be simplified, but still should take into account the real displacements in the most relevant joints and the natural ground reaction forces during real gait foot loading [8, 18]. Foot loading is important to activate the relevant brain and spinal cord neuronal circuits underlying stepping movements [6, 7], however, it also increases the required actuators' force range.

To safely generate high forces, pneumatic actuation is the optimal choice in the MR-environment: besides an easy handling of large forces with high dynamics over a wide range of motion, pneumatic actuators are compliant and can be switched to a safe moveable state with zero pneumatic force by connecting the chambers to the atmosphere. Furthermore, disturbing ferromagnetic and electronic components such as valves and control units can remain outside of the scanner room, while only the air tubes are guided to the pneumatic cylinders [35]. In addition, no hygienic problems occur in the case of leakage, which is of special relevance in the clinical environment of MR scanners. However, the non-linearities in the pneumatic components and the very long tubes create dead time and delay (i.e. low-pass filter) effects. Furthermore, MR compatible cylinder and piston materials may introduce large friction that makes the control of pneumatic systems very challenging. In addition, the system's behavior changes between subjects due to subject-individual limb masses and lengths, and joint viscoelasticity. Therefore, purely model-based controllers would require extensive model parameter identification to provide reproducible movements and, thus, reproducible brain activation for each individual subject.

In this work, we present an iterative learning controller (ILC) [2] and a performance-based adaptive control [10] to improve the usability of our magnetic resonance compatible stepper (MARCOS) with pneumatic actuation [18].

2 Methods

2.1 Hardware setup

MARCOS can move the legs of a subject in supine position in an MRI scanner. The subject is fixed with a pillow at the back in combination with a stiff hip belt, shoulder belts and an adapted head bowl [18]. The feet of the subject are each placed in a shoe and fixed with Velcro® fasteners. The shoe can slide on a linear guide. A pneumatic cylinder attached to a knee orthoses can move the knee up and down (Fig. 1). The resulting movement resembles on-the-spot stepping, including displacements at the hip, knee and ankle joints. At each leg, a second pneumatic cylinder is attached to the shoe on the linear guide. This second cylinder allows the control of a force at the foot sole, simulating ground reaction forces.

Proportional way valves (MPYE, Festo, Germany) control the air flow to the knee cylinders. These valves remain outside of the scanner room. The air is guided via 7 m long air tubes to the cylinders inside the scanner room. The cylinders attached to the shoes are controlled with pressure control valves (VPPM, Festo, Germany). The position of each cylinder is redundantly measured by potentiometers and optical encoders. The forces are measured with resistive strain gauges (Transmetra Gmbh, Switzerland) attached to aluminum substrate at the end of each cylinder.

The materials used in the design of MARCOS were limited to PVC, aluminum and brass, as these materials are characterized by a low magnetic susceptibility. During fMRI measurements, all force and position signals that are measured inside the scanner room are collected inside a shielded aluminum box and guided outside via fiber-optic cable. The current supply is provided with DC current inside a shielded cable connected to the shielding of the scanner room.

2.2 Control

MARCOS can work in three different modes: (i) subject-passive mode, i.e. the subject remains passive, (ii) subject-active

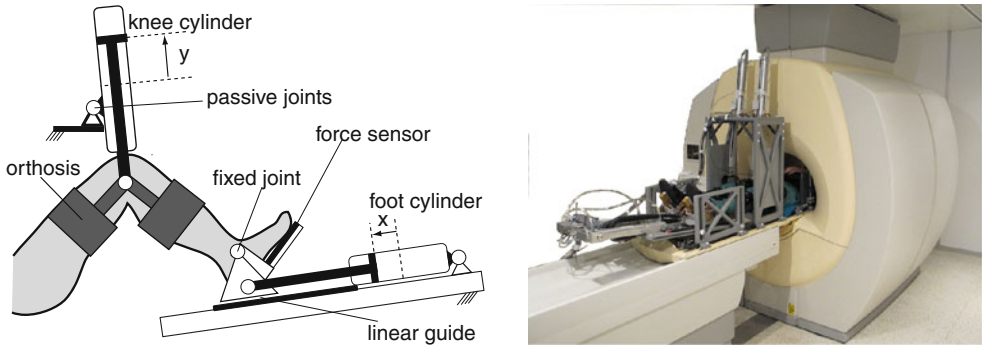

Fig. 1 *Left* principle sketch of MARCOS [18]. Cylinders at the knee and the foot guide one degree of freedom leg movement with control of position and force at the foot. *Right* MARCOS in the fMRI scanner

mode, i.e. the subject has to move, and (iii) assist-as-needed mode, i.e. assistance by the robot is provided only when the subject individual needs require it. In all modes, the force that acts on each foot is controlled independently with the foot cylinders (Fig. 1) to impose a specified profile. This independent control is possible due to the redundancy of the system: the kinematic constraints allow movement only in one degree of freedom, so that each leg is over-actuated.

2.3 Subject-passive mode

The subject-passive mode combines feedback position and force controllers with an iterative learning feed-forward controller, exploiting the cyclic nature of the task. The position controller enforces the desired knee trajectory by controlling the position of the cylinder that is attached to the knee (y coordinate in Fig. 1) by the cylinder's proportional flow valves. The controller output $\hat{u}_{\text{pos}}$ (valve opening) is proportional to the difference between the desired knee position y_{ref} and the measured position y_{meas} with a proportional gain P_{pos} $(m-1)$:

$$\hat{u}_{\text{pos}} = P_{\text{pos}}(y_{\text{ref}} - y_{\text{meas}}). \tag{1}$$

One side effect of proportional valves is their non-linear behavior. To partially compensate this, the controller output $\hat{u}_{\text{pos}}$ is transformed into actuator input u_{pos} using a linear function with dead zone, since there is no noticeable flow for input values lower than 0.03 (± 0.5 corresponds to a completely open valve, 0 to a closed valve):

$$u_{\text{pos}} = \begin{cases} 0, & \hat{u}_{\text{pos}} = 0 \\ \hat{u}_{\text{pos}} - 0.03, & \hat{u}_{\text{pos}} < 0 \\ \hat{u}_{\text{pos}} + 0.03, & \hat{u}_{\text{pos}} > 0 \end{cases} \tag{2}$$

The force control at the foot has a cascaded structure (Fig. 2). An inner pressure control loop is performed directly by proportional pressure control valves. The reference pressure u_{footCyl} is calculated using an outer proportional force controller with additional feed-forward terms

$$u_{\text{footCyl}} = (F_{\text{ref}} + P_{\text{foot}}(F_{\text{ref}} - F_{\text{meas}}) + pF_{\text{ref}}x)/A \tag{3}$$

with desired foot force F_{des}, measured force F_{meas}, proportional gain P_{foot}, piston area A, piston displacement x (Fig. 1), and a manually tuned constant factor p. The term $pF_{\text{ref}}x$ approximately compensates for the dependency of pressure build-up on chamber volume, resulting in a simplified version of the control strategy as suggested in [31]. The factors p and P_{foot} were chosen ad hoc.

The two cylinders at each leg are mechanically coupled through the human leg. Thus, forces from one cylinder have an impact on the performance of the other cylinder. Because limb masses, limb lengths, and joint viscoelasticities differ between subjects, and since the attachment of the knee orthoses is also variable, the characteristics of this coupling change between subjects. To compensate for these model uncertainties in these particular repetitive movements, the feedback controllers are combined with an ILC [2]. The ILC compensates not only for the mutual influence of the two actuators, but also for all repeating disturbances, e.g. non-linearities at the valves, tubes, cylinders, as well as friction and inertial forces. For each leg, the ILC outputs a two-dimensional feed-forward control vector $u_{\text{k}}(t)$ $((1,\ \text{Pa})-1)$ for the current cycle k as a function of time t (at the beginning of each cycle, time t is reset to zero). The entries of this vector correspond to the two knee cylinders (for position control) and the two foot cylinders (for force control). This control output is re-calculated from cycle to cycle, using the control signal $u_{k-1}(t)$ that was applied during the preceding cycle $k-1$ and the corresponding four-dimensional (two positions, two forces) error trajectory $e_{k-1}(t)$ $((\text{m},\ \text{N})^{-1})$. The previous control output $u_{k-1}(t)$ is pre-multiplied by a two-by-two "forgetting matrix" $\mathbf{Q}$, whereas the corresponding error trajectory $e_{\text{k}-1}(t)$ is shifted in time by Δt and then pre-multiplied by the diagonal two-by-two "learning matrix" $\mathbf{P}_{\text{ILC}}$:

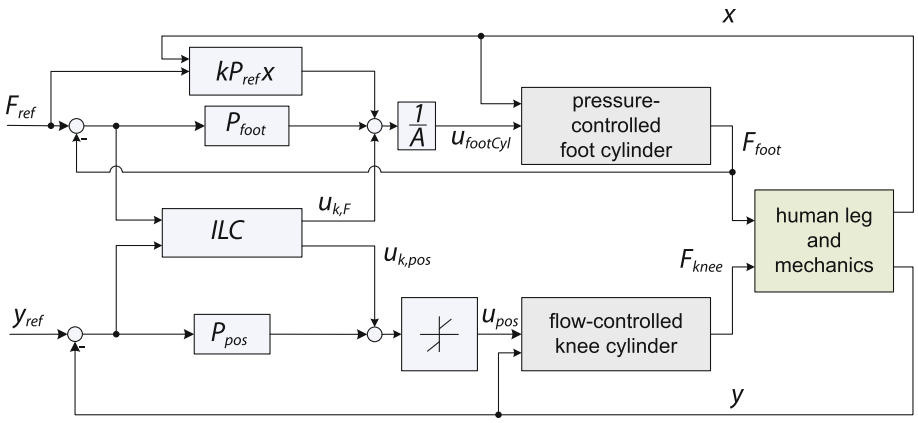

Fig. 2 Control chart for the subject-passive control mode

$$u_k(t) = \mathbf{Q}u_{k-1}(t) + \mathbf{P}_{\mathrm{ILC}}e_{k-1}(t + \Delta t). \quad (4)$$

The matrix structure of the ILC allows the coupling of the system. However, for simplicity, the matrices were chosen to be diagonal. Still, the cross-coupling of the actuating variables is taken into account over their time dependency. The diagonal values of the forgetting matrix $\mathbf{Q}$ were chosen to be 0.9. The learning matrix $\mathbf{P}_{\mathrm{ILC}}$ is also diagonal, with gains 0.7 for position and 0.2 for force errors. The time shift Δt was manually adjusted to compensate for the delay in the reaction time of the system (position controller: $\Delta t = 0.15$ s; force controller $\Delta t = 0.05$ s).

The calculated feed-forward control signal $u_k(t)$ is added to the output of the position and force feedback controllers (Fig. 2).

2.4 Subject-active mode

In subject-active mode, the robot follows the movements of the subject in such a way that interaction forces between the legs and the knee orthoses are minimal. Thus, the robot is compliant and the subject can achieve any physiological knee position y. To this end, the force at each knee $F_{\mathrm{meas,knee}}$ is controlled to be constant, only counteracting the gravitational force W (N) resulting from the weight of the orthosis (0.8 kg).

This force control is achieved by a proportional force feedback with gain P_1 The non-linearity resulting from the varying chamber size is taken into account by adding the term $P_2 \times F_{\mathrm{meas,knee}}$. We further added a quadratic term in the force $P_3\left(W - F_{\mathrm{meas,knee}}\right)^2$ to increase the control output as larger the force was:

$$u_{\mathrm{knee}} = (P_1 + P_2 x)\Big((W - F_{\mathrm{meas,knee}}) + P_3(W - F_{\mathrm{meas,knee}})^2\Big). \quad (5)$$

The force feedback control for the foot cylinder remains unchanged. However, no ILC is used because the subject controls the movement, and thus disturbances are no longer predictable.

2.5 Assist-as-needed mode

The subject-passive mode does not allow subjects to try the task by themselves, and thus reduces the subject's effort. On the other hand, the subject-active mode requires the subject to have sufficient motor ability to move the robot, which is not possible for individuals who have reduced functional movement.

It would be desirable to include the safety aspects and the accurate trajectory demonstration of the subject-passive mode, while still allowing participants to try the movement by themselves. One strategy is to provide less guidance as practice progresses based on real-time measures of subject performance. Several adaptive strategies have been proposed of the form:

$$R_{k+1} = f_{\mathrm{R}}R_k - g_{\mathrm{R}}\left|x_k - x_{d,k}\right| \quad (6)$$

where R_k is the control parameter that is adapted (e.g. the robot stiffness), k refers to the kth cycle, f_{R} is the robot forgetting factor, g_{R} is the robot learning gain, x_k is the performance variable (e.g. measured position) and $x_{d,k}$ is the desired performance variable (e.g. desired position). If f_{R} is chosen such that $0 < f_{\mathrm{R}} < 1$, then the error-based learning algorithm reduces the control parameter when the performance error $\left|x_k(t) - x_{d,k}(t)\right|$ is small, with the effect of always challenging the patient.

Such a controller was modified in [11] to adjust the impedance gains of a walking assisting robot at different points of the step trajectory during walking training of spinal cord injured subjects. However, to adjust the gain parameters of an impedance-based controller is only viable when working with a very backdriveable robot [11]. Pneumatically driven robots are intrinsically not back-driveable, and thus, when the assistance is reduced to zero,

even healthy subjects still require an excessive amount of force to influence the robot.

Our goal is to define an adaptive controller able to provide mechanically compliant assistance during the movement, while still allowing the subject to be challenged. Here, we suggest a modification of the Eq. (6) based on the ILC Eq. (4) introduced above: the desired assistive force is adapted, instead of a control parameter as the impedance gain, based on the tracking error:

$$F_{d,k}(t) = f_{\mathrm{R}} F_{d,k-1}(t) + g_{\mathrm{R}}\big(x_k(t) - x_{d,k}(t)\big). \quad (7)$$

This adaptive law adjusts the assisting force at the knee cylinder F_d, for the current cycle k as a function of time t (t is reset to zero at the beginning of each cycle), using the desired force of the previous cycle $F_{d,k-1}(t)$ and the tracking error in the current cycle $\left|x_k(t) - x_{d,k}(t)\right|$. The robot forgetting factor is denoted as f_{R} ($f_{\mathrm{R}} = 0.98$), g_{R} is the robot learning gain ($g_{\mathrm{R}} = 50$), x_k is the current knee position and $x_{d,k}$ is the desired knee position.

The desired force F_d is re-calculated from cycle to cycle at each sample time and input to a close-loop force controller similar to the one described in Eq. (5).

$$u_{\mathrm{knee}} = (P_1 + P_2 x)\big((F_d + W - F_{\mathrm{meas,knee}}) + P_3 (F_d + W - F_{\mathrm{meas,knee}})^2\big) \quad (8)$$

3 Experimental protocol

3.1 Subject-passive mode

The controllers for the subject-passive and the subject-active modes were tested outside of the scanner on seven healthy subjects (p1–p7 in Table 1). The study was approved by the local ethical committee and conducted in compliance with the Declaration of Helsinki. Informed consent was obtained from each subject before the evaluation session.

For subject-passive mode, sinusoidal trajectories at 0.5 Hz were predefined for both the force on the foot sole (0–200 N) and the knee position (0.01–0.17 m). First, MARCOS effected three movement cycles without ILC. Thereafter, the iterative learning started and lasted over 30 movement cycles. Then, learning was stopped, and the final feed-forward trajectory continued to be added to the controller signals for ten more cycles. In the end, the feed-forward signals were set to zero and ten cycles were performed.

In order to evaluate the benefit of the ILC in the control performance, the phase shift between the maxima of the desired and measured trajectories for position and force was analyzed, as well as the movement variability. The learning progress in reducing the time shift was analyzed with a Friedman test followed by a Bonferroni adjustment (data were not normal distributed, tested with a Kolmogorov–Smirnov test). Significance level was set to 0.05.

Table 1 Information of healthy subjects

Subject	Age	Height (cm)	Weight (kg)	BMI	Gender
p1	29	179	72	22.5	Male
p2	29	170	80	27.7	Male
p3	28	182	74	25	Female
p4	31	183	87	26	Male
p5	29	183	68	20.3	Male
p6	27	182	65	19.6	Male
p7	26	179	60	18.7	Female
a1	22	172	73	24.7	Male
a2	25	185	65	19	Male
a3	32	180	68	21	Male
a4	23	182	72	21.7	Male
f1	24	169	63	22.1	Female
f2	23	182	72	22.7	Male

BMI stands for body mass index

3.2 Subject-active mode

The controller performance for the subject-active mode was evaluated by measuring the maximal reaction forces between the cylinder and the knee orthoses. The subjects were asked to move freely with a similar amplitude and frequency as during the passive mode for 15 cycles.

3.3 Assist-as-needed mode

The assist-as-needed mode was tested with three healthy subjects outside the scanner (a1–a3 in Table 1). In order to measure subject effort (i.e. subject self-generated force production), electromyography (EMG) signals were recorded from four muscles of the dominant leg: rectus femoris, biceps femoris, tibialis anterior and medial gastrocnemius. EMG data were acquired with a wireless system (TELEMYO$^{\mathrm{TM}}$ 2400T Direct Transmission System, Noraxon, USA) at 1,500 Hz. Disposable, self-adhesive dual Ag/AgCl snap electrodes were used. EMG data were rectified and smoothed in Matlab with a time window of 50 ms. All EMG data were finally normalized with respect of the maximum voluntary contraction of each muscle.

Subjects were requested to move their dominant leg to try to match their knee position (represented on a computer screen by a moving blue bar), to the desired knee position (green bar). The desired trajectory was defined as a sinusoidal trajectory of 0.5 Hz with knee position ranging from

0.01 to 0.17 m. During the EMG test, no load was applied on the subjects' foot sole. A foot load facilitates the knee flexion, and thus the effect of reducing the assistance could have been masked by an increase of load on the foot.

All the three control modes were tested. In each mode, nine trials were recorded. Each trial consisted of 30 s of moving followed by a rest phase of 10 s. All subjects started in subject-passive mode in order to allow the subject to understand the task. They were requested to relax their legs. The order of the two other modes was randomized. Before the assist-as-needed mode started, the controller learned the force profile needed to track the desired knee position while subjects were completely passive (during 40–70 cycles, depending on the subject). Then, the assist-as-needed mode started and subjects were instructed to be always active. Subjects were not informed about the fading of the assistance.

After the desired force profile was successfully learned for ten cycles, the absolute tracking error, the mean assisting force, and mean EMG of the four muscles per trial were measured. To test the correlation between assisting force and EMG activation, a Pearson's correlation test for each subject was performed. EMG activation levels were further compared between modes.

One subject was tested outside the scanner (a4 in Table 1) to evaluate the performance of the assist-as-needed controller when a sinusoidal load was applied on the foot sole (0–200 N).

3.4 fMRI pilot study

A pilot study with two healthy subjects (f1 and f2 in Table 1) was performed in the MR-Center of University of Zurich, on a Philips Achieva 1.5T MR system equipped with an 8 channel SENSETM head coil. Subjects performed the same protocol as described above for the EMG experiment under all three different control modes.

The functional acquisitions used a T2* weighted, single shot, field echo, echo-planar-imaging (EPI) sequence of the whole brain (TR = 3 s, TE = 50 ms, flip angle = 82°, FOV = 220 × 220 mm^2, acquisition matrix = 128 × 128, inplane resolution = 1.7 × 1.7 mm^2, slice thickness = 3.8 mm, SENSE factor 1.6, 35 slices). Image processing and analysis were performed using SPM8. Functional images were normalized into standard stereotactic space using the Montreal Neurological Institute template (MNI). The data analysis (t test, $p < 0.001$) was performed on a subject-by-subject basis to identify the activated neuronal network involved in each training mode, compared to the rest periods.

4 Results

4.1 Subject-passive mode

Both the median value and the variability of the phase shift during position control with ILC were smaller than during position feedback control only (Fig. 3). After 30 learning cycles, the median of the phase shift of one cycle was significantly reduced from 0.283 s (10/90 percentile: 0.0775 s) to 0.054 s (10/90 percentile: 0.016 s, Wilcoxon test, $p = 0.015$). From the eighth cycle onwards, the time shift no longer differs significantly from any following time shifts. This corresponds to 38 s for movements performed with a frequency of 0.5 Hz. The inclusion of the ILC reduced the maximal positioning error to 6.5 mm. The maximal variability (10/90 percentile) of the movement was reduced by 84 % from 0.0415 m without the ILC to 0.0065 m with the ILC.

The force controller with the ILC also reached a smaller maximal variability (maximal 10/90 percentile: 15 N, without ILC: 44 N) than the feedback-controller alone (Fig. 4).

4.2 Subject-active mode

The controller for subject-active mode kept the interaction forces between knee orthosis and leg smaller than 20 N (desired: 0 N) (Fig. 5) at an operating force range of

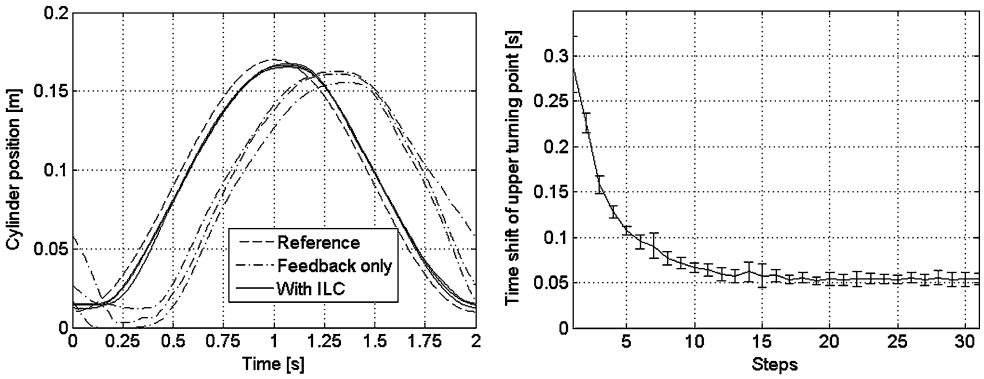

Fig. 3 *Left* knee position (y): mean and 10/90 percentile of 10 cycles from the left leg of seven subjects. 0.2 m corresponds to a knee angle of approx. 50°. *Right* the time shift and 10/90 percentile of the upper turning point plotted over the learning iterations

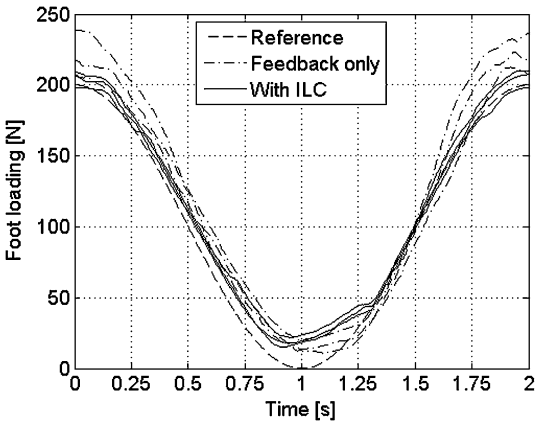

Fig. 4 The median (and 10/90 percentile) of the force at the foot. Displayed are the median of 10 cycles before and 10 cycles after 30 learning cycles of all seven subjects

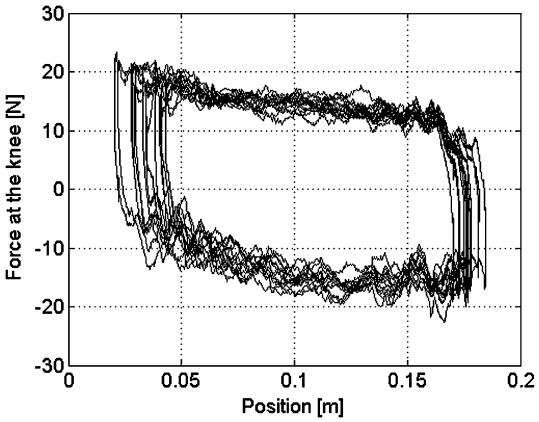

Fig. 5 Reaction force at the knee for the active mode for the voluntary movement of one subject over 10 cycles plotted over the position

0–200 N. For comparison, in the uncontrolled case (valves open), the reaction forces are around 100 N (reduction of 80 %).

The force control in subject-active mode has the same performance as during subject-passive mode, as it is independent from the knee movements.

4.3 Assist-as-needed mode

The median and 10/90 percentile range of the absolute value of the tracking error was calculated after the force profile to move the leg in passive form was successfully learned for 10 cycles for the three subjects (Fig. 6, left). The mean tracking error was 0.0163 m (10/90 percentile: 0.0296 m). The mean phase shift was 0.0688 s (10/90 percentile: 0.1563 s), in the order of the phase shifts observed in the subject-passive mode. The values of the median tracking error and phase shift during 10 cycles of the subject performing with the sinusoidal load on the foot were in the same order of magnitude (median tracking error: 0.0095 m, 10/90 percentile: 0.0429 m; phase shift median: 0 s, 10/90 percentile: 0.0438 s).

During the assist-as-needed test, the mean assistance force provided by the robot systematically decreased as the subjects performed the task without experiencing large tracking errors (Fig. 6, right). Each subject showed a different faded assistance curve, dependent on the tracking errors created during the test and the initial value of the assistive force. The final assistance level in the plateau was also different for each subject and never identical to zero.

In all subjects, the mean EMG activity of the biceps femoris significantly correlated with the assistance force (Fig. 7 up, Pearson's correlation test: a1 $R = -0.886$, $p = 0.002$; a2 $R = -0.741$, $p = 0.026$; a3 $R = -0.691$, $p = 0.039$). Even if subjects were instructed to actively try to follow the desired knee position from the first trial, the EMG activity increased as less assistance was provided to the subject. Besides the biceps femoris, no other muscle consistently correlated with the assistance force.

The EMG activation levels of the biceps femoris were further compared between modes. The mean EMG activation increased at each trial, starting at a level close to the mean EMG recorded during subject-passive mode, towards more activation as recorded during the subject-active mode (Fig. 7, down).

4.4 fMRI pilot study

Over all modes and subjects, maximal translational head motion was within an acceptable range (<2.5 mm) in the inferior/superior direction. A conjunction analysis from the two healthy subjects showed significant neuronal activation in all three experimental conditions. Active stepping of the right leg elicited significant activation in an extensive sensorimotor network including medial primary motor areas and premotor areas in the left cerebral hemisphere as well as activation in the Vermis and the right hemisphere of the Cerebellum. Passive stepping elicited activation in medial primary motor areas and premotor areas in the left cerebral hemisphere but not the cerebellum. Stepping with assist-as-needed led to significant activations in the left primary sensorimotor areas and bilaterally in the superior parietal lobe. Furthermore, the Vermis and the right cerebellar hemisphere were significantly activated (Fig. 8).

5 Discussion

An iterative learning controller was implemented to guarantee high repeatability of movements. The ILC learning time of eight cycles is short, and thus the controller setup time prior to the intended fMRI measurements will not be

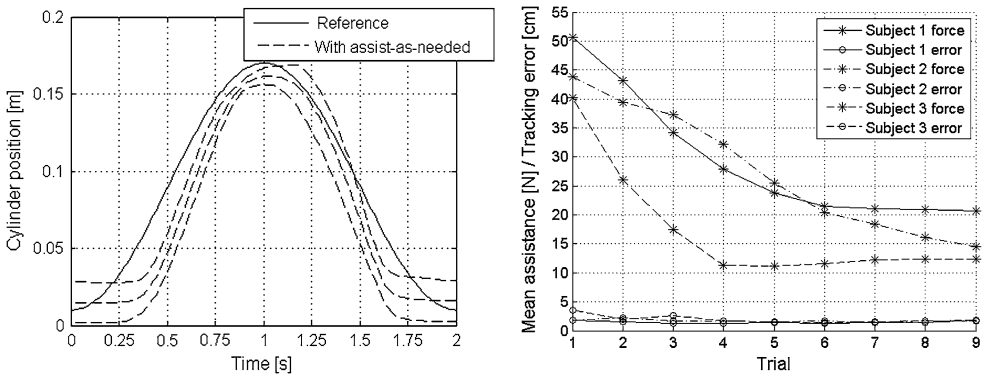

Fig. 6 *Left* mean and SD of the knee position of 10 cycles from the right leg. *Right* fading of the assisting force provided by the robot as the subjects performed the task

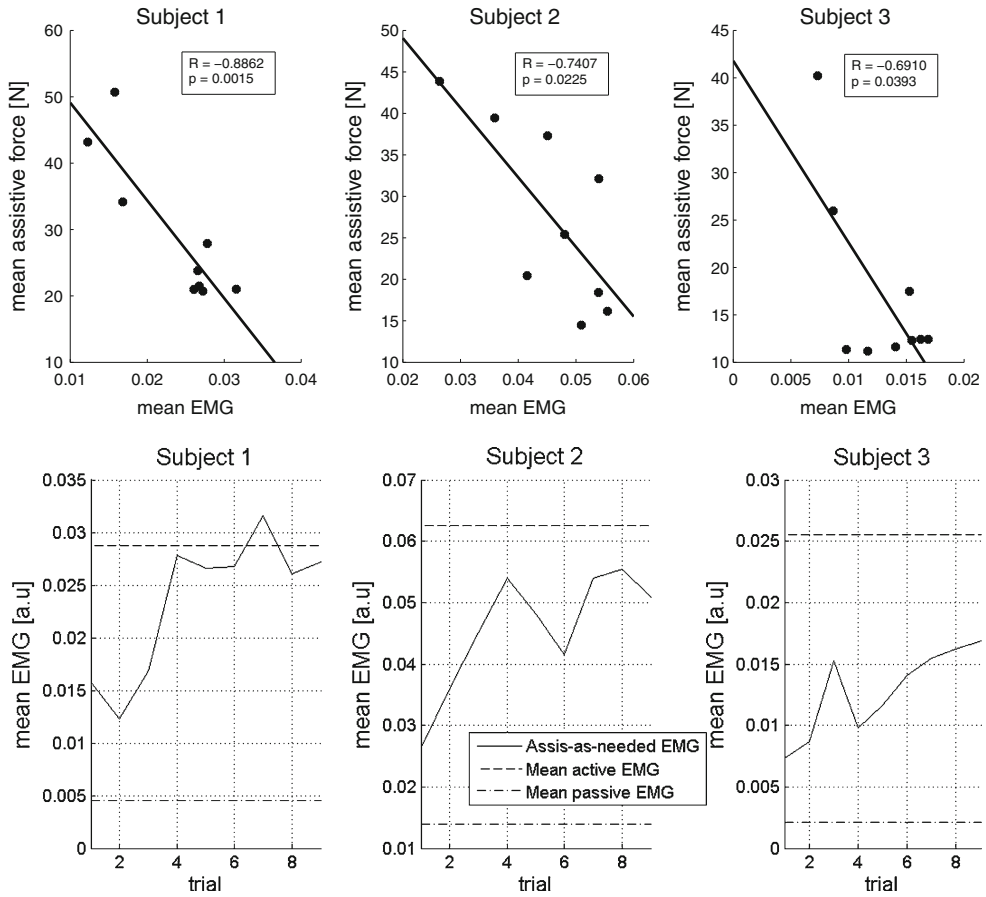

Fig. 7 *Up* correlation between mean biceps femoris EMG activity and the mean assistive force from the robot. *Down* mean biceps femoris EMG evolution during the experiment

considerably extended, while the control performance is significantly improved. The maximal positioning error after the inclusion of the ILC does not affect the fMRI results, as it is relatively small (6.5 mm) compared to the human movement range. In addition, the movement variability between subjects was also significantly reduced. The performance of the classic feedback force controller was already satisfactory, and thus no further improvement was observed with the inclusion of the ILC (although we found that the variability between subjects was reduced). The performance differences between the classic force and position feedback controllers might be due to the different control strategies that aim at controlling the pressure in force feedback, and the air flow in position control.

Proving passivity of a system like MARCOS is challenging: approaches using linear models are not sufficient to capture the non-linear nature of an MR-compatible pneumatic system such as MARCOS. Formulating a suitable non-linear model is also not possible due to the excessive parameter uncertainties and time invariances,

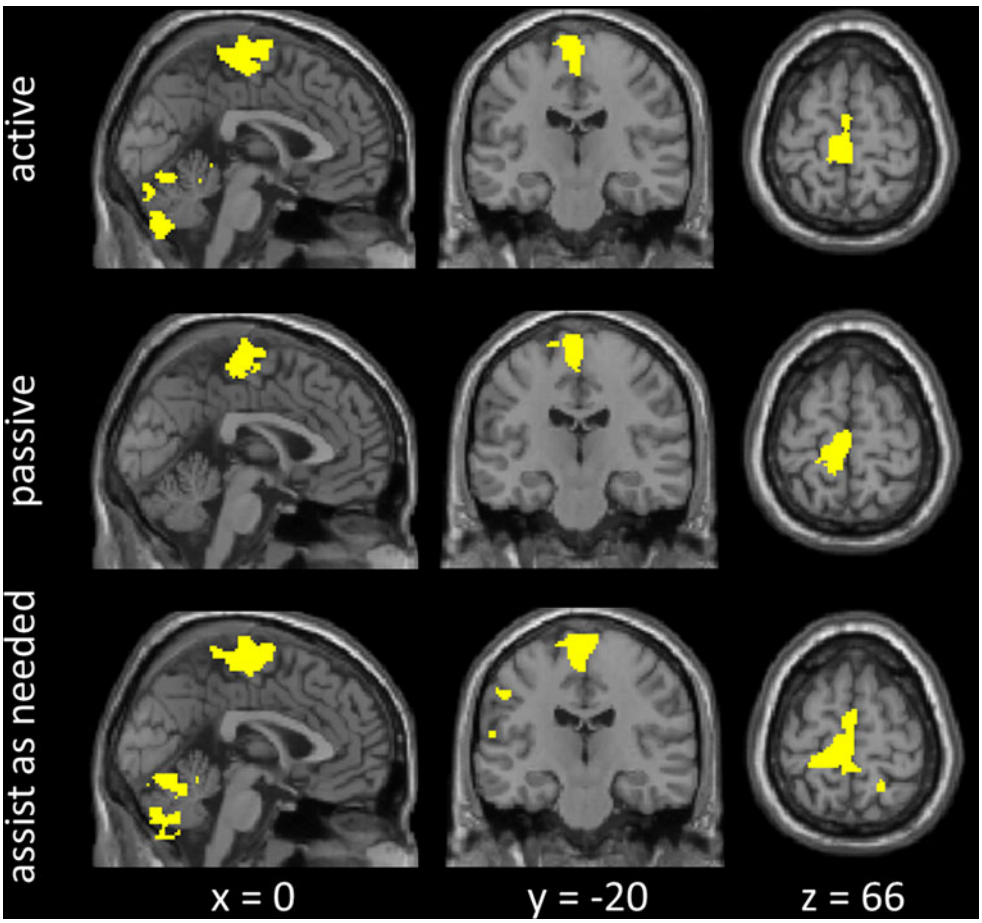

Fig. 8 Clusters of significant neuronal activation during active, passive and assist-as-needed stepping of the right leg. All images are $p \leq 0.001$, uncorrected $k = 42$ voxels, coordinates are in MNI space

which are a consequence of the chosen mechanical concept. Due to varying biomechanical properties between subjects, also the set-up of the robot varies between subjects. Robust control strategies have been proposed to account for high uncertainties affecting dynamical systems. However, robust control is associated with performance degradation as a higher level of robustness is required. These challenges in modeling and the cyclic nature of the task were the main reasons for applying an ILC.

The robustness and stability were empirically tested disturbing the robot and checking its satisfactory robust response. To guarantee safety, the actuator outputs were limited, as well as their rate of change over time. In addition, all position sensor signals are measured redundantly to detect sensor failure. Forces that exceed the safety limits would immediately trigger an emergency stop: chambers are then connected to the atmosphere, and thus, the robot is set into a moveable state.

In subject-active mode, subjects had to overcome maximal reaction forces of up to 20 N at the knee. This force is low in comparison to the leg weight of about 150 N. The assist-as-needed algorithm was able to adapt the robot assistance step by step while subjects were passively moved by the robot. We note that although the mean phase shift was in the order of the values observed in the subject-passive mode, the tracking was not perfect. This is due to the forgetting factor ($f_R = 0.98$): the assistance force converged into a steady state that corresponded with an amount of assistance slightly lower than the least amount the subject needed to achieve the movement. When the subjects were instructed to actively perform the task, the assistance systematically decreased as the subjects performed without experiencing large tracking errors till an unperceived amount. However, it was never equal to zero, due to the subjects' natural variability. The assist-as-needed controller performed as expected to encourage subject's effort: EMG activation in the biceps femoris increased as the assistance force was systematically reduced, even if the subjects were instructed to be always active. A consistent correlation between muscle activity and assistance in any other leg muscles was not found. This was expected, as only the biceps femoris is involved in

knee flexion, while most subjects use the help from the gravity force to extent the leg.

Results from the fMRI pilot study indicate that the controllers are suitable to evoke substantial neural activation in a network of the brain known to be involved in sensorimotor control of the legs without introducing artifacts at cerebral level. Further experiments with a larger number of subjects are necessary to examine the underlying mechanisms in further detail.

In conclusion, we recommend using pneumatics in combination with the controllers presented here to provide a safe actuation principle and a good control performance.

Acknowledgments This work was supported in part by the EMDO foundation, Koster foundation, International foundation of paraplegia, and the Swiss National Science Foundation (SNF). Laura Marchal-Crespo holds a Marie Curie International income fellowship PIIF-GA-2010-272289. We thank Alessandro Rotta and Andreas Brunschweiler for their support in machining and assembling of MARCOS, Andrew Pennycott for proofreading, and Jasmin Schneider for her support with EMG recordings.

References

1. Bakker M, Verstappen CCP, Bloem BR, Toni I (2007) Recent advances in functional neuroimaging of gait. J Neural Transm 114(10):1323–1331
2. Bristow DA, Tharayil M, Alleyne AG (2006) A survey of iterative learning control. Control Syst IEEE 26(3):96–114
3. Chapuis D, Gassert R, Ganesh G, Burdet E, Bleuler H (2006) Investigation of a cable transmission for the actuation of MR compatible haptic interfaces. In: Proceedings 1st International Conference on Biomedical Robotics and Biomechatronics, IEEE/RAS- EMBS, Italy, pp 426–431
4. Chinzei K, Hata N, Jolesz FA, Kikinis R (2000) Surgical assist robot for the active navigation in the intraoperative MRI: hardware design issues. In: Proceedings International Conference on Intelligent Robots and Systems, IEEE/RSJ, Japan, pp 727–732
5. Dan S, Alexandru P, Doru P, Dumitru M, Louis K (2007) A new type of motor: pneumatic step motor. IEEE/ASME Trans Mechatron 12(1):98–106
6. Dietz V, Gollhofer A, Kleiber M, Trippel M (1992) Regulation of bipedal stance: dependency on "load" receptors. Exp Brain Res 89(1):229–231
7. Dietz V, Duysens J (2000) Significance of load receptor input during locomotion: a review. Gait Posture 11(2):102–110
8. Dietz V, Muller R, Colombo G (2002) Locomotor activity in spinal man: significance of afferent input from joint and load receptors. Brain 125(12):2626–2634
9. DiMaio SP, Pieper S, Chinzei K, Hata N, Haker SJ, Kacher DF, Fichtinger G, Tempany CM, Kikinis R (2007) Robot-assisted needle placement in open MRI: system architecture, integration and validation. Comput Aided Surg 12(1):15–24
10. Emken JL, Benitez R, Reinkensmeyer DJ (2007) Human-robot cooperative movement training: learning a novel sensory motor transformation during walking with robotic assistance-as-needed. J Neuroeng Rehabil 4:8
11. Emken JL, Harkema SJ, Beres-Jones J, Ferreira CK, Reinkensmeyer DJ (2008) Feasibility of manual teach-and-replay and continuous impedance shaping for robotic locomotor training following spinal cord injury. IEEE Trans Biomed Eng 55:322–334
12. Fennessy FM, Tuncali K, Morrison PR, Tempany CM (2010) MR imaging-guided interventions in the genitourinary tract: an evolving concept. Magn Reson Imaging Clin N Am 18(1):11–28
13. Fischer GS, Iordachita I, Csoma C, Tokuda J, DiMaio SP, Tempany CM, Hata N, Fichtinger G (2008) MRI-compatible pneumatic robot for transperineal prostate needle placement. IEEE/ASME Trans Mechatron 13(3):295–305
14. Flueckiger M, Bullo M, Chapuis D, Gassert R, Perriard Y (2005) fMRI compatible haptic interface actuated with traveling wave ultrasonic motor. In: Proceedings Industry Applications Conference, IEE/IAS, Hong Kong, pp 2075–2082
15. Ganesh G, Gassert R, Burdet E, Bleuler H (2004) Dynamics and control of an MRI compatible master-slave system with hydrostatic transmission. In: Proceedings International Conference on Robotics and Automation, IEEE, New Orleans, pp 1288–1294
16. Gassert R, Moser R, Burdet E, Bleuler H (2006) MRI/fMRI-compatible robotic system with force feedback for interaction with human motion. IEEE/ASME Trans Mechatron 11(2): 216–224
17. Hempel E, Fischer H, Gumb L, Höhn T, Krause H, Voges U, Breitwieser H, Gutmann B, Durke J, Bock M, Melzer A (2003) An MRI-compatible surgical robot for precise radiological interventions. Comput Aided Surg 8(4):180–191
18. Hollnagel C, Brügger M, Vallery H, Wolf P, Dietz V, Kollias S, Riener R (2011) Brain activity during stepping: a novel MRI-compatible device. J Neurosci Methods 201(1):124–130
19. Israel JF, Campbell DD, Kahn JH, Hornby TG (2006) Metabolic costs and muscle activity patterns during robotic- and therapist-assisted treadmill walking in individuals with incomplete spinal cord injury. Phys Ther 86(11):1466–1478
20. Khanicheh A, Muto A, Triantafyllou C, Weinberg B, Astrakas L, Tzika A, Mavroidis C (2006) fMRI-compatible rehabilitation hand device. J NeuroEng Rehabil 3(1):24
21. Khanicheh A, Mintzopoulos D, Weinberg B, Tzika AA, Mavroidis C (2008) MR_CHIROD v. 2: magnetic resonance compatible smart hand rehabilitation device for brain imaging. IEEE Trans Neural Syst Rehabil Eng 16(1):91–98
22. Lotze M, Braun C, Birbaumer N, Anders S, Cohen LG (2003) Motor learning elicited by voluntary drive. Brain 126(4):866–872
23. Marchal-Crespo L, Reinkensmeyer D (2009) Review of control strategies for robotic movement training after neurologic injury. J NeuroEng Rehabil 6(1):20
24. Marchal-Crespo L, McHughen SA, Cramer SC, Reinkensmeyer DJ (2010) The effect of aging and haptic guidance on motor learning of a steering task. Exp Brain Res 201(2):209–220
25. Perez MA, Lungholt BK, Nyborg K, Nielsen JB (2004) Motor skill training induces changes in the excitability of the leg cortical area in healthy humans. Exp Brain Res 159(2):197–205
26. Pondman KM, Fütterer JJ, ten Haken B, Schultze Kool LJ, Witjes JA, Hambrock T, Macura KJ, Barentsz JO (2008) MR-guided biopsy of the prostate: an overview of techniques and a systematic review. Eur Urol 54(3):517–527
27. Riener R, Lunenburger L, Jezernik S, Anderschitz JM, Colombo G, Dietz V (2005) Patient-cooperative strategies for robot-aided treadmill training: first experimental results. IEEE Trans Neural Syst Rehabil Eng 13(3):380–394
28. Riener R, Villgrattner T, Kleiser R, Nef T, Kollias S (2005) fMRI-compatible electromagnetic haptic interface. In: Proceedings 27th Annual International Conference of the Engineering in Medicine and Biology Society, IEEE-EMBS, Shanghai, pp 7024–7027
29. Timmermans AA, Seelen HAM, Willmann RD, Kingma H (2009) Technology-assisted training of arm-hand skills in stroke: concepts on reacquisition of motor control and therapist guidelines for rehabilitation technology design. J NeuroEng Rehabil 6:1

30. Tsekos NV, Khanicheh A, Christoforou E, Mavroidis C (2007) Magnetic resonance-compatible robotic and mechatronics systems for image-guided interventions and rehabilitation: a review study. Annu Rev Biomed Eng 9(1):351–387
31. Xiang F, Wikander J (2004) Block-oriented approximate feedback linearization for control of pneumatic actuator system. Control Eng Pract 12(4):387–399
32. Yu NB, Riener R (2006) Review on MR-compatible robotic systems. Proceedings 1st International Conference on Biomedical Robotics and Biomechatronics, IEEE/RAS-EMBS, New York, pp 722–726
33. Yu N, Murr W, Blickenstorfer A, Kollias S, Riener R (2007) An fMRI compatible haptic interface with pneumatic actuation. In: Proceedings 10th International Conference on Rehabilitation Robotics, IEEE, Netherlands, pp 714–720
34. Yu N, Hollnagel C, Blickenstorfer A, Kollias S, Riener R (2008) fMRI-compatible robotic interfaces with fluidic actuation. In: Robotics: Science and Systems Conference, Zurich
35. Yu N, Hollnagel C, Blickenstorfer A, Kollias S, Riener R (2008) Comparison of MRI-compatible mechatronic systems with hydrodynamic and pneumatic actuation. IEEE/ASME Trans Mechatron 13(3):268–277